J. Biochem. 2012;152(1):45–52 doi:10.1093/jb/mvs050

JB THE JOURNAL OF BIOCHEMISTRY

The crystal structure of an intermediate dimer of aspergilloglutamic peptidase that mimics the enzyme-activation product complex produced upon autoproteolysis

Received September 16, 2011; accepted March 3, 2012; published online May 7, 2012

Hiroshi Sasaki[1,2,*], Keiko Kubota[3,*], Woo C. Lee[3,*], Jun Ohtsuka[3,*], Masaki Kojima[4], So Iwata[5,6], Atsushi Nakagawa[7], Kenji Takahashi[1,4,†] and Masaru Tanokura[1,3,‡]

[1]Department of Biophysics and Biochemistry, Graduate School of Science, The University of Tokyo, 7-3-1 Hongo, Bunkyo-ku, Tokyo 113-0033, Japan; [2]Tokiwa Junior College, 1-430-1 Miwa, Mito, Ibaraki 310-8585, Japan; [3]Department of Applied Biological Chemistry, Graduate School of Agricultural and Life Sciences, The University of Tokyo, 1-1-1 Yayoi, Bunkyo-ku, Tokyo 113-8657, Japan; [4]School of Life Sciences, Tokyo University of Pharmacy and Life Sciences, 1432-1 Horinouchi, Hachioji, Tokyo 192-0392, Japan; [5]Department of Biological Sciences, Imperial College, London SW7 2AZ, England; [6]Institute of Materials Structure Science, High Energy Accelerator Research Organization, 1-1 Oho, Tsukuba, Ibaraki 305-0801, Japan and [7]Institute of Protein Research, Osaka University, 3-2 Yamadaoka, Suita, Osaka 565-0871, Japan

*These authors contributed equally to this work.

[†]Kenji Takahashi, School of Life Sciences, Tokyo University of Pharmacy and Life Sciences, 1432-1 Horinouchi, Hachioji, Tokyo 192-0392, Japan. Tel: +81 49 297 3308, Fax: +81 49 297 8168, email: kenjitak@toyaku.ac.jp

‡Masaru Tanokura, Department of Applied Biological Chemistry, Graduate School of Agricultural and Life Sciences, The University of Tokyo, 1-1-1 Yayoi, Bunkyo-ku, Tokyo 113-8657, Japan. Tel: +81 3 5841 5165, Fax: +81 3 5841 8023, email: amtanok@mail.ecc.u-tokyo.ac.jp

Aspergilloglutamic peptidase from *Aspergillus niger* var. *macrosporus* (AGP) is one of the so-called pepstatin-insensitive acid endopeptidases, which are distinct from the well-studied aspartic peptidases. Among the known homologues of the glutamic peptidases, AGP is a unique two-chain enzyme with a light chain and a heavy chain bound non-covalently with each other, and thus is an interesting target for protein structure–function relationship studies. In this article, we report the crystal structure of a dimeric form of the enzyme at a resolution of 1.6 Å. This form has a unique structure in which the C-terminal region of the light chain of one of the molecules binds to the active site cleft of the other molecule like a part of a substrate. This form mimics the enzyme-activation product complex produced upon autoproteolysis, and provides a structural clue that could help to clarify the activation mechanism. This type of dimeric structure of a peptidase is here reported for the first time.

Keywords: aspergilloglutamic peptidase/*Aspergillus niger*/crystal structure/enzyme–product complex/glutamic peptidase.

Abbreviations: AGP, aspergilloglutamic peptidase; H chain, heavy chain; L chain, light chain; RMSD, root-mean-square deviation; SGP, scytalidoglutamic peptidase; 3D, three-dimensional.

Aspergilloglutamic peptidase (AGP; MEROPS ID: G01.002; formerly called aspergillopepsin II or *Aspergillus niger* proteinase A) is a pepstatin-insensitive acid endopeptidase produced by the fungus *Aspergillus niger* var. *macrosporus* (*1*, *2*) and belongs to the newly established family of glutamic peptidases (*i.e.* peptidase family G1). It is known to be synthesized as a 282-residue preproenzyme with a 59-residue prepro sequence at the N-terminus and an intervening 11-residue sequence (*3*), and then activated autocatalytically to the mature enzyme under acidic conditions. The mature AGP is a two-chain enzyme with a 39-residue light (L) chain and a 173-residue heavy (H) chain bound non-covalently with each other (*4*). This primary structure is different from those of the other glutamic peptidase homologues identified so far, which are composed of a single chain. The H chain is cross-linked by three intramolecular disulphide bonds. It is active under acidic conditions like pepsin and other aspartic peptidases, but is insensitive to their specific inhibitors, such as pepstatin, diazoacetyl-D,L-norleucine methyl ester/Cu^{2+} ions, and 1,2-epoxy-3-(*p*-nitrophenoxy)propane. Furthermore, our site-directed mutagenesis studies (*5*, *6*) demonstrated that Glu110 in the H chain (Glu110H) is essential for the catalytic activity. Based on these results, we suggested that Glu110H is one of the catalytic residues and that the enzyme may be called a glutamic proteinase (*6*). We also reported the crystal structure of AGP in the type I crystals at 1.4-Å resolution (PDB code 1Y43) (*7*), and showed that Gln24H is also one of the critical residues in the enzyme by site-directed mutagenesis studies (*8*). These results indicate that the enzyme should be a glutamic peptidase with a Glu–Gln catalytic dyad. The crystal structures of scytalidoglutamic peptidase (SGP; MEROPS ID: G01.001), an AGP homologue, were also determined (PDB codes 1S2B, 1S2K, 2IFW and 2IFR) (*9*, *10*), and the catalytic mechanism with a Glu–Gln catalytic dyad of SGP was proposed (*10*). However, the three-dimensional (3D) structure mechanism for the AGP-specific autoprocessing has never been clarified. In this article, we describe in detail the dimeric structure of AGP in the type III crystal form determined by X-ray crystallography at a resolution of 1.6 Å. This form has a unique structure composed of two AGP molecules in an

asymmetric unit, where the C-terminal region of the L chain of one of the molecules is bound to the active site cleft of the other molecule like a part of a substrate.

Materials and Methods

Protein purification and crystallization

AGP was purified from the crude extract powder (Proctase, Meiji Seika Co., Tokyo) obtained from the culture filtrate of *A. niger* var. *macrosporus* (*2*). Crystals of the dimeric AGP ($0.1 \times 0.2 \times 0.2$ mm^3, type III crystal) were obtained by the hanging-drop vapour diffusion method in 3 months with a reservoir solution containing 1.3 M ammonium sulphate, 0.1 M glycine buffer (pH 2.5–2.75) and 5% (v/v) dimethyl sulphoxide at 4°C (*11*).

Diffraction data collection

The crystals were mounted in a glass capillary and the X-ray diffraction data were collected at room temperature at BL6A at the Photon Factory. Data were processed using the program HKL 2000 (*12*). Data collection statistics are summarized in Table I.

Model building and refinement

The structure of type III AGP (*i.e.* AGP III) was solved by the molecular replacement method using the program MOLREP (*13*) with the structure of type I AGP crystal (*i.e.* AGP I) (PDB code 1Y43), which is a monomer, as the initial model. The initial model was constructed by using XtalView (*14*) and Coot (*15*) and refined with the program REFMAC5 (*16*). The water molecules were added using ARP/wARP (*17*). The qualities of the models were checked by RAMPAGE (*18*). The refinement statistics are shown in Table I. Atomic coordinates and structure factors for AGP III have been deposited in the Protein Data Bank with the accession code 3TRS.

Table I. Data collection and refinement statistics for AGP III.

Crystals	
Beamline	PF-BL6A
Wavelength (Å)	1.000
Resolution (Å)[a]	50.1–1.60 (1.64–1.60)
Space group	$P2_12_12_1$
Unit-cell parameters (Å)	$a = 60.69$
	$b = 65.84$
	$c = 77.39$
Molecules per asymmetric unit	2
No. of unique reflections	37,983
Completeness (%)[a]	95.9 (85.5)
$\langle I \rangle / \langle \sigma (I) \rangle$[a]	12.3 (3.2)
R_{merge}[a,b]	0.071 (0.309)
Refinement	
Resolution (Å)	38.7–1.60
R_{work}	0.208
R_{free}[c]	0.239
RMSDs	
Bond length (Å)	0.019
Bond angle (°)	1.925
Average *B* factors (Å^2)	
Overall	16.38
Protein	15.63
Water oxygen	26.60
Dimethyl sulphoxide	46.22
Ramachandran plot	
Favoured region (%)	97.8
Allowed region (%)	2.2
Outlier region (%)	0.0

[a]The values in parentheses are for the highest resolution shell.
[b]$R_{merge} = \Sigma_{hkl}\Sigma_i|I_i(hkl) - \langle I(hkl)\rangle|/\Sigma_{hkl}\Sigma_i\ I_i(hkl)$, where $I_i(hkl)$ is the *i*th intensity measurement of reflection *hkl*, including symmetry-related reflections and $\langle I(hkl)\rangle$ is its average.
[c]R_{free} was calculated from 5% of reflections omitted from the refinement.

Model analyses

Superimposition of protein models and calculation of the average root-mean-square deviations (RMSDs) were performed using the program Swiss-PDB Viewer (*19*). The PISA server (*20*) was used for calculation of the buried surface area. All figures were produced by the program PyMOL (*21*).

Results

X-ray crystallographic analysis of the dimeric AGP

The crystal structure of the dimeric AGP has been determined at a resolution of 1.6 Å (Fig. 1). Table I shows the crystallographic parameters. It belonged to space group $P2_12_12_1$, and the final crystallographic *R*-factor was 20.8% (R_{free}, 23.9%). All the non-glycine residues lie in the energetically most favoured and additionally allowed regions in the Ramachandran plot (*22*). The final $2F_o$–F_c map showed continuous and well-defined electron densities for the protein atoms, except for the following regions. For each of the protomers (designated as AGP-A and AGP-B) of the dimeric AGP, the N-terminal Glu1 and the C-terminal Tyr39 of the L chain and the N-terminal pyrGlu1–Ser2 sequence of the H chain of AGP-A and the N-terminal Glu1 and the C-terminal Val32–Tyr39 sequence of the L chain and the N-terminal pyrGlu1–Ser–Glu3 sequence of the H chain of AGP-B were not seen in the electron density map.

Structure of the dimeric AGP

Figure 1 shows the structure of the dimeric AGP III containing two molecules of AGP per asymmetric unit. These two protomers were bound with each other in a specific manner, and the interfaces between the two protomers had a total buried surface area of 11,480 Å^2. Each protomer had essentially the same 3D structure as that in the type I crystals; however, the C-terminal tail of the L chain (Val32L–Gly38L) of AGP-A was visible except for the C-terminal Tyr39L, and extended out of the molecule to bind to the active site groove of the other molecule (AGP-B) like the enzyme-activation product complex produced upon autoproteolysis. The average RMSD between the two protomers was 0.57 Å for 200 superimposed C^α atoms. The RMSD between AGP-A and AGP I was 0.72 Å for 202 superposed C^α atoms and that between AGP-B and AGP I was 0.98 Å for 200 superposed C^α atoms.

The dimeric structure seems to be stabilized by hydrogen bonding and hydrophobic interactions at two interfaces. As shown in Fig. 2, one of the interfaces includes interactions with nine hydrogen bonds between the two protomers. For this interaction, AGP-A provided three strands (β12, β12a and β16a) and four loops (the C- and N-terminal loops of the L and H chains, respectively, and the β7–β8 and β12–β12a loops) and AGP-B provided three strands (β6, β7 and β10) and two loops (β6–β7 and β12–β12a). Interestingly, this interface includes a Tyr-rich sequence, Tyr42H-X-X-Tyr45H-X-X-Tyr48H-X-Tyr50H of AGP-B. All of these Tyr residues except for Tyr45H are involved in hydrogen bonding with several other residues on the interface. The side chain of Tyr42H in AGP-B binds to those of Asp116H and Ser117H in AGP-A. In addition, the

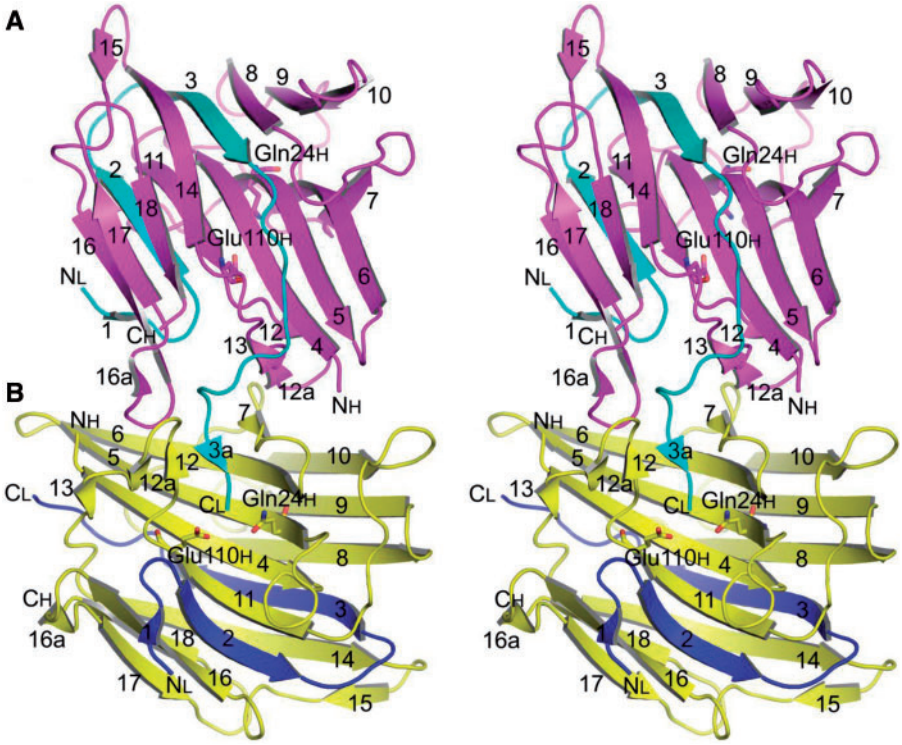

Fig. 1 Stereoview of the crystal structure of a dimeric form of AGP (AGP III). The structure is shown in a ribbon model. The upper and lower protomers are designated as AGP-A and AGP-B, respectively. The light and heavy chains (L and H chains) of AGP-A are shown in cyan and magenta, respectively; and those of AGP-B are shown in blue and yellow, respectively. The β-strands are numbered from the N-terminus to the C-terminus. The structure includes two short β-strands 12a and 16a in addition to the 18 strands found in AGP type I (*7*). NL and CL indicate the N- and C-termini respectively, of the L chain, and NH and CH those of the H chain. The catalytic residues, Glu110H and Gln24H, are shown in a stick model. The oxygen and nitrogen atoms are coloured red and blue, respectively, as in all subsequent figures, unless otherwise specified. The residues in the L chain and H chain were designated by placing L and H, respectively, following the residue numbers. All these notations are used in this article, unless otherwise specified.

side chains of His90H and Ser53H in AGP-B bind to that of Asp116H and those of Glu113H and Leu118H, respectively in AGP-A. These interactions should stabilize the loop β12–β12a of AGP-A. On the other hand, the side chain of Tyr50H and the main chain NH group of Tyr48H in AGP-B bind to that of Glu3H in AGP-A, and the side chain of Tyr48H in AGP-B binds to that of Ser33L in AGP-A. These interactions should also contribute to the binding of the two protomers.

As shown in Fig. 3, the other interface includes at least eight hydrogen bonds between the two protomers. The electron densities at the C-terminus of the L chain reveal that Gly38L adopts two conformations: the major conformation (Gly38AL) in which the C-terminal carboxylate interacts with Ser8H and the minor conformation (Gly38BL) in which the carboxylate interacts with Gln24H (Figs 3, 5, 6 and 8A–D). For this interface, AGP-A provided one loop (β16–β16a) and a C-terminal tetrapeptide (Gly35L–Ser–Ser–Gly38L) of the L chain involving one strand (β3a), and AGP-B provided one loop (β12–β12a) and six strands (β4–β7, β11 and β12). The peptide chain NH and CO groups of the C-terminal tetrapeptide are hydrogen-bonded to the side chains or peptide chain CO and NH groups, respectively of eight residues of AGP-B (Ser8H, Gln24H, Asp28H, Glu43H, Ala49H, Glu110H, Glu113H and Gly115H) and one residue of AGP-A (Asp154H). Among these residues, Asp28H, Glu110H and Asp154H are hydrogen

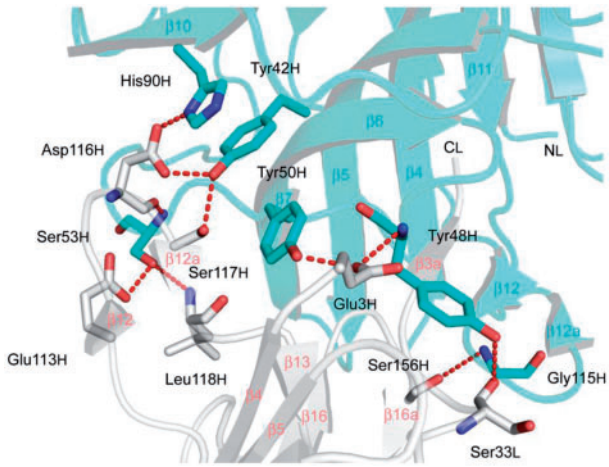

Fig. 2 The first interface between AGP-A (carbon, white) and AGP-B (carbon, cyan). The amino acid side chains involved in the interactions are shown in a stick model. Hydrogen bonds are shown as red dotted lines.

bonded to the tetrapeptide moiety through interaction with water molecules.

Active site structure

As described above, the C-terminal tetrapeptide portion of the AGP-A L chain binds to the active site cleft

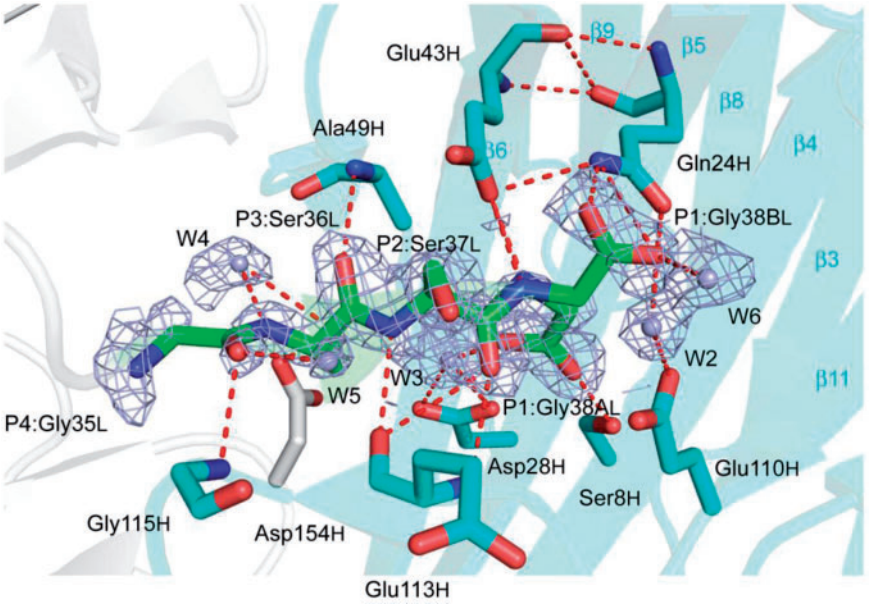

Fig. 3 The second interface between AGP-A and AGP-B. The C-terminal tail (Gly–Ser–Ser–Gly; carbon, green) of the L chain of AGP-A with the $2F_o–F_c$ electron density map and the residues (carbon, cyan and white) in AGP-B involved in its binding are shown. The water molecules (light purple spheres) are also shown. Hydrogen bonds are shown as dotted lines. The residue numbers of the C-terminal tail are shown with the P1–P4 designation. The same expressions as used in this panel are used in all subsequent figures unless otherwise specified.

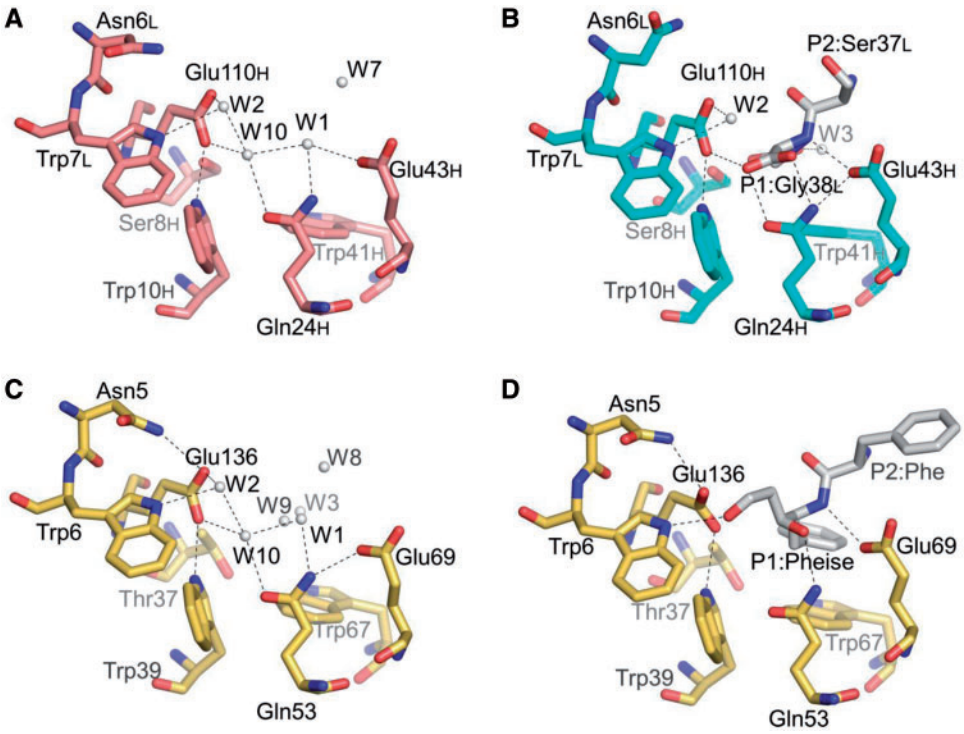

Fig. 4 Catalytic site structure of AGP and its comparison with that of SGP. (A) AGP I (carbon, pink). (B) AGP-B (carbon, cyan) complexed with the C-terminal tail of AGP-A (carbon, white). (C) SGP (carbon, beige, PDB code 1S2B). (D) SGP (carbon, beige) complexed with its inhibitor TA1 (carbon, white, PDB code 2IFW). The water molecules are shown in white spheres.

of AGP-B like a part of a substrate peptide. Judging from the position of the tetrapeptide relative to the catalytic dyad (Fig. 3), Gly35L, Ser36L, Ser37L and Gly38L of the tetrapeptide are thought to correspond to the P4, P3, P2 and P1 residues, respectively of a substrate peptide. Among these residues, Gly35L is hydrogen bonded with Gly115H and W5; Ser36L with Ala49H, Asp154H and W4; Ser37L with

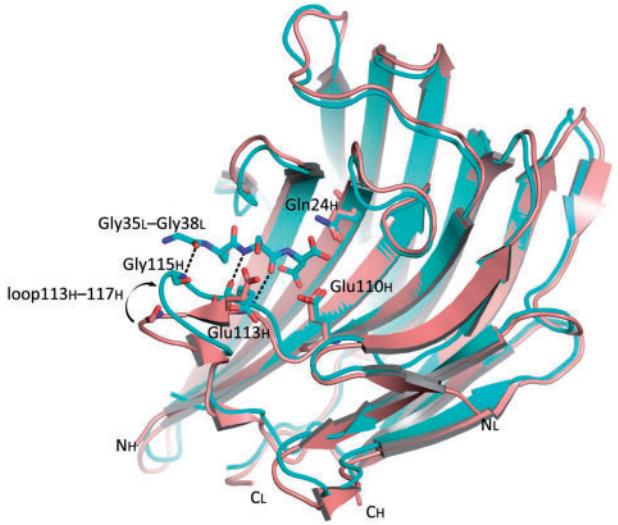

Fig. 5 Overlay of AGP-B with AGP I. The structures of AGP-B and AGP I (PDB code 1Y43) are coloured cyan and pink, respectively. The C-terminal tail of the AGP-A L chain (carbon, cyan) is also shown. The arrow indicates the movement of the loop 113H–117H.

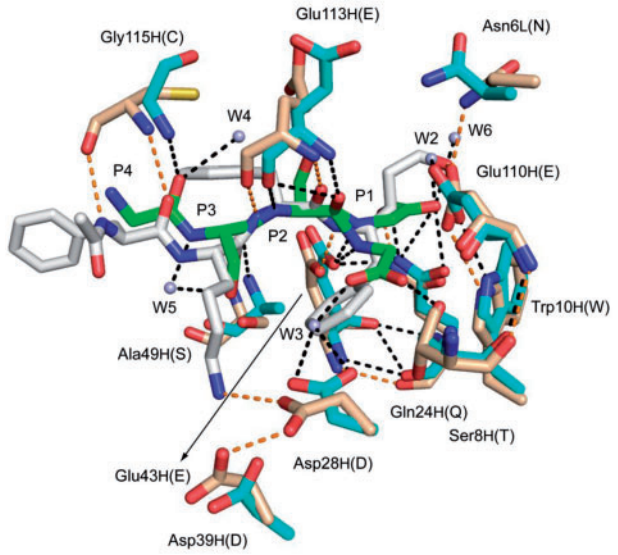

Fig. 6 Overlay of the active site region in AGP-B interacting with the C-terminal tail of the AGP-A L chain and the corresponding region interacting with the synthetic inhibitor TP1 with SGP. The carbon atoms of the C-terminal tail of the AGP-A L chain and the synthetic inhibitor TP1 and SGP are shown in green, white and beige, respectively.

Glu113H; Gly38AL with Ser8H, Glu43H and W3; and Gly38BL with Gln24H, Glu43H, W2 and W6. These residues are thought to constitute part of the S4–S1 sites. Although several residues are involved in the binding, it is noteworthy that none of the side chains of the tetrapeptide moiety are involved in hydrogen bonding to AGP-B.

Figure 4B shows the catalytic site of AGP-B into which the two-residue C-terminal sequence, Ser37L–Gly38L, of the AGP-A L chain was introduced. There was only a subtle difference in the spatial arrangement of the constituent residues between the structures shown in Fig 4A and B, except that the orientation of the side chain of Asn6L was changed. In the presence of Ser37L–Gly38L, however, the water molecules W1, W7 and W10 disappeared, possibly due to introduction of the dipeptide portion from AGP-A into the catalytic site, and a new water molecule, W3, appeared near Trp41H.

Discussion

The dimeric structure of AGP found in this study is unique, since the C-terminal tail of the L chain of one (AGP-A) of the enzyme molecules binds to the active site cleft of the other enzyme molecule (AGP-B) like part of a substrate, presumably mimicking the enzyme-activation product complex produced upon autoproteolysis. Therefore, it provides a structural clue that can help us to understand the activation mechanism. This type of dimeric structure of a peptidase has never been reported previously. The large buried surface area of 11,480 Å^2 indicates that the dimer may be stable in solution. At present, however, we have no additional data to confirm this, and further studies are warranted.

Figure 5 shows a structural comparison of AGP-B with another crystal form of AGP, *i.e.* AGP I. The structure of AGP-B is almost identical with that of AGP I except for the structural change in the loop region, Glu113H-Ser117H. In AGP-B, the side chain of Glu113H changes its direction. This should eliminate the steric hindrance due to the side chain of Glu113H against the entrance of the C-terminal tail of the L chain of AGP-A, permitting the loop to come closer to the active site groove to participate in the P4 residue (Gly35L) recognition by Gly115H. This structural change is thought to be caused mainly by the specific binding of the C-terminal tail of the L chain of AGP-A to the active site groove of AGP-B.

The C-terminal 6–8 residues sequence of the L chain was not clearly seen in the electron density maps of AGP, except for AGP-A. This indicates that this region is normally fluctuating rather freely. Unexpectedly, the C-terminal Tyr of the L chain was found to be missing in AGP-A. Presumably, this residue was removed by the action of a carboxypeptidase (*23*) present in the culture medium of *A. niger* var. *macrosporus* after maturation of AGP. The contents of proteolytic enzymes in the culture medium of this fungus, including this carboxypeptidase, are known to change significantly due to changes in the cultivation conditions. Indeed, various changes in cultivation conditions have been made occasionally by the manufacturer in the cultivation of this fungus to raise the yields of other enzymes, especially aspergillopepsin I. Presumably, the sample of AGP used in this study was prepared from a lot of the crude extract powder with a high carboxypeptidase content. In this connection, it should be noted that the activation of recombinant AGP zymogen at pH 3.5, where no contaminating peptidase is present, proceeds in a step-wise fashion, and the final maturation involves the cleavage after the C-terminal Tyr (Tyr39L) of the L chain; thus, the

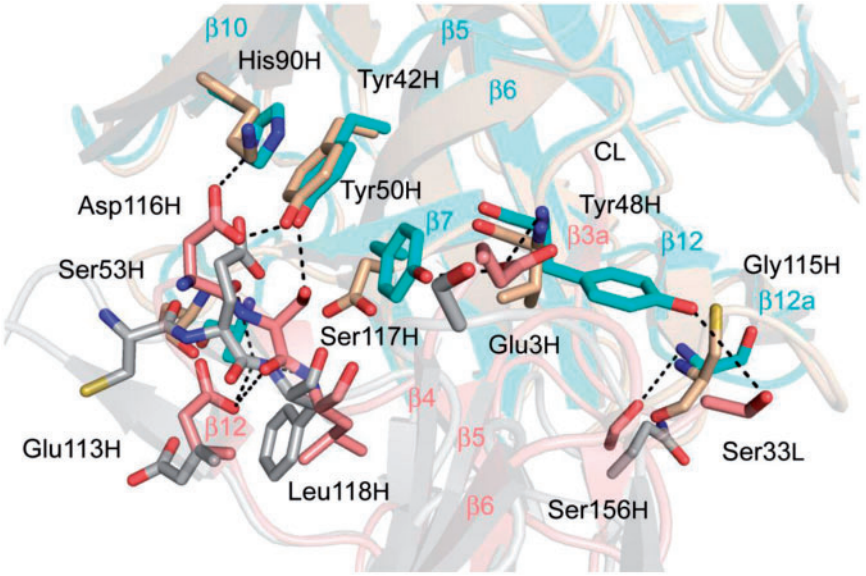

Fig. 7 Overlay of the interface region between AGP-B and AGP-A and the hypothetical interface region of SGP corresponding to that of AGP-B and AGP-A. The carbon atoms in AGP-A and AGP-B are shown in pink and cyan, respectively. The carbon atoms in the hypothetical interface region of SGP corresponding to that of AGP-A and AGP-B are shown in grey and beige, respectively.

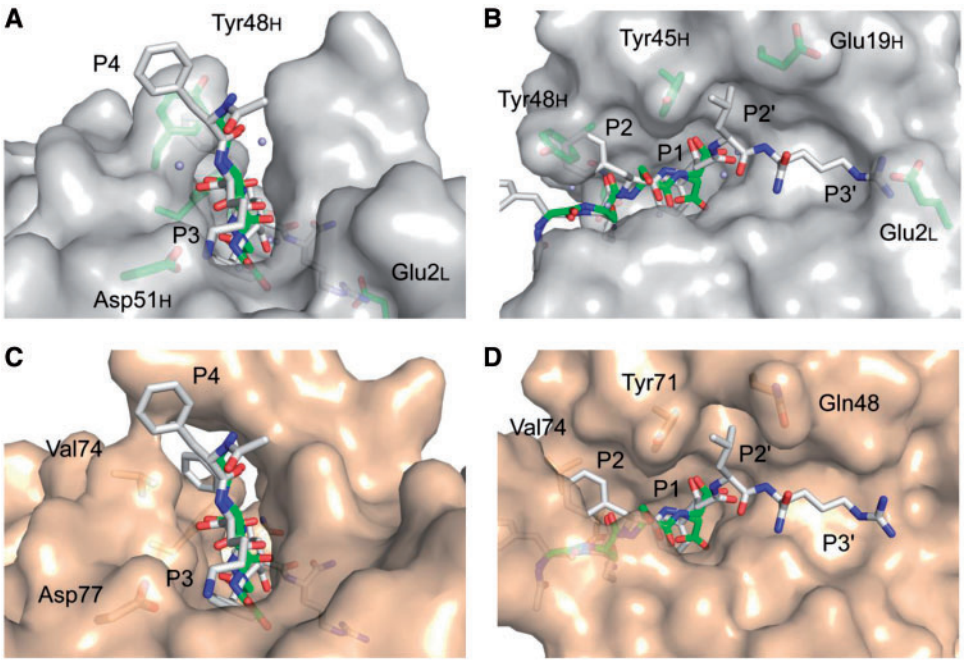

Fig. 8 Comparison of the active site groove structures of AGP-B and SGP, and the mode of binding of the C-terminal tetrapeptide of AGP-A and the SGP inhibitor TA1. The structures are shown as seen from two different directions for AGP [(A) and (B)] and for SGP [(C) and (D)].

complete 39-residue L chain with the C-terminal Tyr was produced and identified by mass spectrometry as the final L chain (*24*). It should also be noted that the L chain of AGP used previously for primary structure determination had been shown to be the complete 39-residue peptide with the C-terminal Tyr39L (*4*).

The autocatalytic activation of the AGP zymogen is thought to take place by an intermolecular reaction (*24*). The present dimeric form appears to mimic a complex in which the C-terminal tail portion of the L chain of one AGP molecule (AGP-A), as an activation cleavage product, binds to the active site groove of another AGP molecule (AGP-B) in the process of autoproteolysis. Actually, the dimeric form is thought to be formed by rebinding of the two activated AGP molecules. In the actual activation, however, Tyr39L should be the P1 residue and come in juxtaposition to the catalytic dyad. Due to the lack of this Tyr residue, Gly38L is thought to occupy this site upon rebinding of the two AGP molecules. This apparent one-residue

shift of the peptide chain along the active site groove is presumably due to the flexibility of the C-terminal tail region of the L chain highly abundant in Gly and Ser residues (–Gly32–Ser–Ser–Gly–Ser–Ser–Gly–Tyr –Gly–Gly–Gly–Tyr43–). In the dimeric AGP, Ser33L and Glu3H of AGP-A are both hydrogen bonded to Tyr48H of AGP-B.

Figure 6 compares the hydrogen-bonding interactions at the active site region of AGP-B with the C-terminal tail (Gly35L–Gly38L) of the AGP-A L chain and of SGP with a synthetic inhibitor, TA1 [Ac-FKF(3*S*,4*S*)-phenylstatinyl-LR-NH_2]. Among the residues shown, eight are identical, including the two catalytic residues, and three are similar (Ser8H versus Thr, Ala49H versus Ser, and Gly115H versus Cys) and have similar positions and orientations. The C-terminal tail of the L chain of AGP-A, and the synthetic inhibitor also overlap well. Thus, the mode of binding of the C-terminal tail of the AGP-A L chain to AGP-B is similar to that of the SGP inhibitor to SGP (*9*, *10*). These results also indicate that the S4–S1 subsites are partially similar between the two enzymes. However, the orientation of the side chain of Asn6L of AGP was changed upon binding of the C-terminal tail of the AGP-A L chain (Fig. 4A and B), whereas no significant change in orientation of the constituent residues in SGP was observed upon binding of the inhibitor TA1 (Fig. 4C and D) (*9*, *10*).

Figure 7 shows the interface between AGP-A and AGP-B (also Fig. 2), where two molecules of SGP are overlapped. In contrast to the active site regions of both enzymes, the structure of this interface region is quite different between AGP and SGP. Among the regions different in 3D structure between AGP and SGP, two regions, Asp51H–Glu59H and Ser114H–Asp116H, are present at or near this interface, and the location and/or orientation is especially different for the side chains in SGP corresponding to those of Glu3H, Tyr48H, Tyr50H, Ser53H, Glu113H, Asp116H and Ser117H. Moreover, in SGP, the side chain of Asp76 corresponding to Tyr50H would collide with that of Ser143, which corresponds to Ser117H, in the other molecule. Taking these differences into consideration, together with the fact that the interaction involving the C-terminal tail of the L chain of AGP is not present in SGP, formation of the dimeric form of AGP is thought to be difficult for SGP, and hence to be unique to AGP.

Figure 8 shows the active site grooves of AGP-B and SGP into which the C-terminal four-residue sequence Gly–Ser–Ser–Gly (35L–38L) of the L chain of AGP-A and the SGP inhibitor, TA1, are fitted. The phenyl group of the P4 Phe of the inhibitor lies outside the groove, free from steric hindrance (Fig. 8A). However, the side chains of the P3 Lys, P2 Phe and P3′ Arg of the inhibitor collide with the side chains of Asp51H, Tyr48H and Glu2L, respectively (Fig. 8A and B). In addition, the side chain of the P2′ Leu of the inhibitor is close to the wall of Tyr45H and Glu19H (Fig. 8B). These results suggest that, as compared with SGP, AGP might prefer substrates with somewhat smaller amino acid residues at the P3, P2, P2′ and/or P3′ positions. The tetrapeptide could be accommodated well in the groove of SGP (Fig. 8C and D). The difference in P/P′-site specificity between AGP and SGP is thought to arise mainly from the difference in the interactions between the side chains of the substrate and the surrounding amino acid residues along the active site groove. To elucidate the substrate specificity of AGP in more detail, however, further systematic studies are necessary, including X-ray analysis of AGP-substrate complexes.

Acknowledgements

We are most grateful to the late Prof. Setsuro Ebashi (National Institute for Physiological Sciences, Okazaki) for his continued encouragement. Thanks are also due to Prof. Noriyoshi Sakabe (Institute of Materials Structure Science, High Energy Accelerator Research Organization, Tsukuba) for his helpful input and assistance. A part of this work was performed using the Station PF-BL6A at the Photon Factory, High Energy Accelerator Research Organization, Tsukuba under the approval of the Photon Factory Program Advisory Committee (Proposal Nos. 91-037 and 93G-061). We also thank Bioscience Laboratories, Meiji Seika Co. (Tokyo) for the generous supply of the crude extract powder of the culture filtrate of *A. niger* var. *macrosporus*.

Funding

Grants-in-aid for Scientific Research from the Ministry of Education, Science, Sports, Culture and Technology of Japan; the Japan Society for Promotion of Science; the National Project on Targeted Proteins Research Program (TPRP) of the Ministry of Education, Science, Sports, Culture and Technology of Japan.

Conflict of interest

None declared.

References

1. Takahashi, K. (2004) Aspergillopepsin II in *Handbook of Proteolytic Enzymes* (Barrett, A.J., Rawlings, N.D., and Woessner, J.F., eds.) Vol. 1, 2nd edn., pp. 221–224, Elsevier Academic Press, London
2. Takahashi, K. (1995) Proteinase A from *Aspergillus niger*. *Meth. Enzymol.* **248**, 146–155
3. Inoue, H., Kimura, T., Makabe, O., and Takahashi, K. (1991) The gene and deduced protein sequences of the zymogen of *Aspergillus niger* acid proteinase A. *J. Biol. Chem.* **266**, 19484–19489
4. Takahashi, K., Inoue, H., Sakai, K., Kohama, T., Kitahara, S., Takashima, K., Tanji, M., Athauda, S.B.P., Takahashi, T., Akanuma, H., Mamiya, G., and Yamasaki, M. (1991) The primary structure of *Aspergillus niger* acid proteinase A. *J. Biol. Chem.* **266**, 19480–19483
5. Takahashi, K., Kagami, N., Huang, X.-P., Kojima, M., and Inoue, H. (1998) *Aspergillus niger acid proteinase A - Structure and function in Aspartic Proteinases; Retroviral and Cellular Enzymes* (James, M.N.G., ed.), pp. 275–282, Plenum Press, New York
6. Huang, X.-P., Kagami, N., Inoue, H., Kojima, M., Kimura, T., Makabe, O., Suzuki, K., and Takahashi, K. (2000) Identification of a glutamic acid and an aspartic acid residue essential for catalytic activity of aspergillopepsin II, a non-pepsin type acid proteinase. *J. Biol. Chem.* **275**, 26607–26614
7. Sasaki, H., Nakagawa, A., Muramatsu, T., Suganuma, M., Sawano, Y., Kojima, M., Kubota, K., Takahashi, K., and Tanokura, M. (2004) The three-dimensional

structure of aspergilloglutamic peptidase from *Aspergillus niger*. *Proc. Japan Acad. Ser. B.* **80**, 435–438
8. Yabuki, Y., Kubota, K., Kojima, M., Inoue, H., and Takahashi, K. (2004) Identification of a glutamine residue essential for catalytic activity of aspergilloglutamic peptidase by site-directed mutagenesis. *FEBS Lett.* **569**, 161–164
9. Fujinaga, M., Cherney, M.M., Oyama, H., Oda, K., and James, M.N.G. (2004) The molecular structure and catalytic mechanism of a novel carboxyl peptidase from *Scytalidium lignicolum*. *Proc. Natl Acad. Sci. USA* **101**, 3364–3369
10. Pillai, B., Cherney, M.M., Hiraga, K., Takada, K., Oda, K., and James, M.N.G. (2007) Crystal structure of scytalidoglutamic peptidase with its first potent inhibitor provides insights into substrate specificity and catalysis. *J. Mol. Biol.* **365**, 343–361
11. Sasaki, H, Tanokura, M, Muramatsu, T, Nakagawa, A, Iwata, S, Hamaya, T, Takizawa, T, Kono, T., and Takahashi, K. (1995) X-ray crystallographic study of a non-pepsin-type acid proteinase, *Aspergillus niger* proteinase A in *Aspartic Proteinases: Structure, Function, Biology and Biomedical Implications* (Takahashi, K., ed.), pp. 605–609, Plenum Press, New York
12. Otwinowski, Z. and Minor, W. (1997) Processing of X-ray diffraction data collected in oscillation mode. *Meth. Enzymol.* **276**, 307–326
13. Vagin, A. and Teplyakov, A. (1997) MOLREP: an automated program for molecular replacement. *J. Appl. Crystallogr.* **30**, 1022–1025
14. McReem, D.E. (1999) XtalView/Xfit—A versatile program for manipulating atomic coordinates and electron density. *J. Struct. Biol.* **125**, 156–165
15. Murshudov, G.N., Vagin, A.A., and Dodson, E.J. (1997) Refinement of macromolecular structures by the maximum-likelihood method. *Acta Crystallogr. D.* **53**, 240–255
16. Perrakis, A., Morris, R., and Lamzin, V. (1999) Automated protein model building combined with iterative structure refinement. *Nat. Struct. Biol.* **6**, 458–463
17. Lovell, S.C., Davis, I.W., Arendall, W.B. III, de Bakker, P.I.W., Word, J.M., Prisant, M.G., Richardson, J.S., and Richardson, D.C. (2003) Structure validation by Calpha geometry: phi, psi and Cbeta deviation. *Proteins* **50**, 437–450
18. Kabsch, W. and Sander, C. (1983) Dictionary of protein secondary structure: pattern recognition of hydrogen-bonded and geometrical features. *Biopolymers* **22**, 2577–25637
19. Guex, N. and Peitsch, M. (1997) SWISS-MODEL and the Swiss-Pdb Viewer: an environment for comparative protein modeling. *Electrophoresis* **18**, 2714–2723
20. Krissinel, E. and Henrick, K. (2007) Inference of macromolecular assemblies from crystalline state. *J. Mol. Biol.* **372**, 774–797
21. DeLano, W.L. (2002) *The PyMOL Molecular Graphics System*. Scientific DeLano, San Carlos, CA
22. Ramakrishnan, C. and Ramachandran, G.N. (1965) Stereochemical criteria for polypeptide and protein chain conformations. II. Allowed conformations for a pair of peptide units. *Biophys. J.* **5**, 909–933
23. Kumagai, I. and Yamasaki, M. (1981) Enzymatic properties of an acid carboxypeptidase from *Aspergillus niger* var. *macrosporus*. *Biochim. Biophys. Acta* **659**, 344–350
24. Huang, X.-P., Yabuki, Y., Kojima, M., Inoue, H., and Takahashi, K. (2007) Activation profile of the zymogen of aspergilloglutamic peptidase. *Biol. Chem.* **388**, 129–133